frontiers in Earth Science

ORIGINAL RESEARCH
published: 08 October 2020
doi: 10.3389/feart.2020.580675

Unveiling Powell Basin's Tectonic Domains and Understanding Its Abnormal Magnetic Anomaly Signature. Is Heat the Key?

M. Catalán[1], Y. M. Martos[2,3], J. Galindo-Zaldivar[4,5], L. F. Perez[6] and F. Bohoyo[7]*

[1]Department of Geophysics, Real Observatorio de la Armada, San Fernando (Cádiz), Spain, [2]Planetary Magnetospheres Laboratory, NASA Goddard Space Flight Center, Greenbelt, MD, United States, [3]Department of Astronomy, University of Maryland, College Park, MD, United States, [4]Department of Geodynamics, Universidad de Granada, Granada, Spain, [5]Instituto Andaluz de Ciencias de La Tierra, CSIC-UGR, Granada, Spain, [6]British Antarctic Survey, NERC, Cambridge, United Kingdom, [7]Instituto Geológico y Minero de España, Madrid, Spain

Rifting of continental lithosphere leading to oceanic basins is a complex process conditioned by different factors such as the rheology and thermal structure of the underlying lithosphere, as well as underlying asthenospheric dynamics. All these processes, which finally lead to oceanic domains, can better be recognized in small oceanic basins. Powell Basin is a small oceanic basin bounded to the north by the South Scotia Ridge, to the east by the South Orkney Microcontinent, and to the west by the Antarctic Peninsula. It was formed between the Oligocene and Miocene, however, its age is not well defined, among other reasons due to the small amplitude of its spreading magnetic anomalies. This basin is an ideal framework to analyze the different rifting and spreading phases, which leads from continental crust to the formation of an oceanic domain through different extensional regimes. To identify the different boundaries during the formation of Powell Basin from the beginning of the rifting until the end of the spreading, we use different data sources: magnetic, gravity, multichannel seismic profiles and bathymetry data. We use seismic and bathymetry data to estimate the Total Tectonic Subsidence. Total Tectonic Subsidence has proven to be useful to delineate the different tectonic regimes present from early rifting to the formation of oceanic seafloor. This result together with magnetic data has been used to delimit the oceanic domain and compare with previous authors' proposals. This method could be applied in any other basin or margin to help delimiting its boundaries. Finally, we analyze the role that an asthenospheric branch intruding from the Scotia Sea played in the evolution of the magnetic anomaly signature on an oceanic basin.

Keywords: heat flow, magnetic anomaly, continent-ocean boundary, Bouguer gravity anomaly, asthenospheric channel, total tectonic subsidence

OPEN ACCESS

Edited by:
Susanne Buiter,
RWTH Aachen University, Germany

Reviewed by:
Graeme Eagles,
Alfred Wegener Institute Helmholtz Centre for Polar and Marine Research (AWI), Germany
Joanne M. Whittaker,
University of Tasmania, Australia

****Correspondence:***
M. Catalán
mcatalan@roa.es

Specialty section:
This article was submitted to Solid Earth Geophysics, a section of the journal Frontiers in Earth Science

Received: *06 July 2020*
Accepted: *04 September 2020*
Published: *08 October 2020*

Citation:
Catalán M, Martos YM, Galindo-Zaldivar J, Perez LF and Bohoyo F (2020) Unveiling Powell Basin's Tectonic Domains and Understanding Its Abnormal Magnetic Anomaly Signature. Is Heat the Key?. Front. Earth Sci. 8:580675. doi: 10.3389/feart.2020.580675

INTRODUCTION

The formation of the Drake Passage is considered a remarkable event in Earth's climate history leading to the formation of several small oceanic basins along its southern part. Powell Basin is a by-product of the opening of the Drake Passage, resulting after the fragmentation of the NE extremity of the Antarctic Peninsula. This basin is characterized by a smooth relief that varies from 3,000 to 2,400 m below sea level (**Figure 1**), in the northwestern sector of Weddell Sea. It constitutes an elliptically shaped oceanic domain bounded by a continental block known as the South Orkney

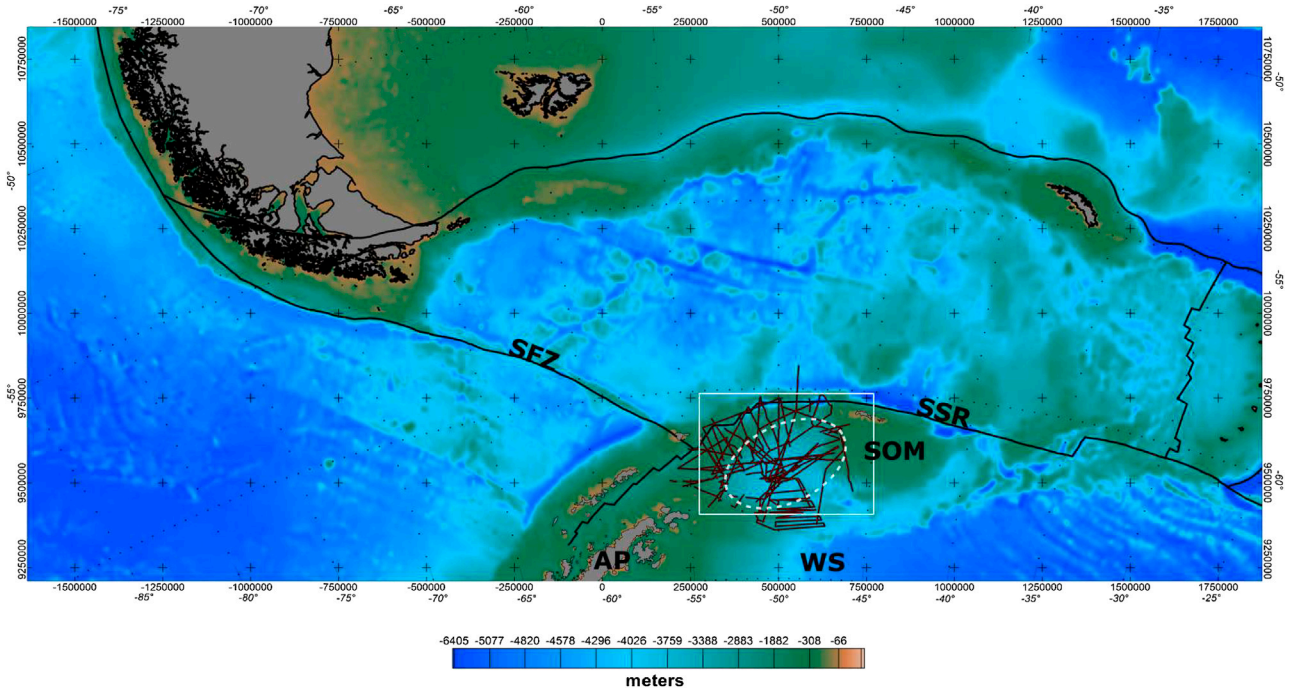

FIGURE 1 | Bathymetry map of the Scotia Sea (SRTM30 Plusv7; Jones et al., 2010). The study area is delimited by a white rectangle. Black lines show the location of MCS profiles used in this study. An elliptical white dotted outline marks Powell Basin's location. AP, Antarctic Peninsula; SFZ, Shackleton Fracture Zone; SSR, South Scotia Ridge; SOM, South Orkney Microcontinent; WS, Weddell Sea.

Microcontinent (SOM) to the east, the South Scotia Ridge (SSR) to the north, and north-western tip of the Antarctic Peninsula to the west. To the south, it is limited by a bathymetric ridge bordering the northern margin of the Weddell Sea.

Powell Basin's Tectonic History

The tectonic history of Powell Basin is not fully understood, although there is a certain agreement regarding its evolution and timing. King and Barker (1988) used a standard age-depth relationship of oceanic lithosphere to support oceanic spreading starting at 29 Ma and finishing at 23 Ma. Lawver et al. (1994), based on heat flow determinations proposed for the formation of the Powell Basin an age around Early Oligocene or Late Eocene (~38–34 Ma). Coren et al. (1997) proposed a three-phase evolution process consisting rifting, drifting and a final rotation based on multichannel seismic profiles and a single marine magnetic profile. They proposed that the final rifting occurred around 27 Ma, followed by a second phase, characterized by asymmetric spreading between the eastern and the western margins, which was active up to 18 Ma. The asymmetric spreading caused a 11° clockwise rotation of the SOM block that finished in the Early Pliocene. Rodríguez-Fernández et al. (1997) proposed oceanic spreading occurring between late Eocene (~38–34 Ma) and early Miocene (23–20 Ma) based on multichannel seismic data. The oceanic spreading occurred through two distinguished phases. During the first phase, the spreading took place mainly in WSW–ENE direction, controlling the eastward drifting of the SOM until it became part of the Antarctic Plate during the Miocene, once the active spreading of the Weddell Sea and Jane Basin ended (Bohoyo et al., 2002). The second phase was largely controlled by thermal subsidence. Eagles and Livermore (2002) proposed for the first time a two-stage formation based on the pattern of magnetic reversals recorded in Powell Basin. As a result, they concluded that the spreading took place between 29.7 and 21.8 Ma, which is close to the proposal made by Coren et al. (1997).

The analysis of small ocean basins such as the Powell Basin constitute an ideal setting for studying the mechanisms that lead to the formation of a new ocean, as well as to analyze the impact caused by different thermal processes such as asthenospheric currents. These are responsible for attracting more and more attention due to their broad implications on plate tectonics. Understanding the variation of the crustal architecture and to determine the continent-ocean boundary are keys to be able to delimit the different tectonic domains. These geological features are poorly known at Powell Basin.

Studies published to date have been based primarily on seismic data. Here, we aim to delimit the different tectonic domains throughout the Ocean-Continent Transition zone (OCTZ), the Continent Ocean Boundary (COB), and then the oceanic domain defined in detail through three types of independent information: gravity, magnetism and total tectonic subsidence (TTS). This information allow us to analyze the oceanic character of the magnetic lineations identified within the basin by Eagles and Livermore (2002) and discuss their origin. To integrate these different sources of information provides a great confidence to

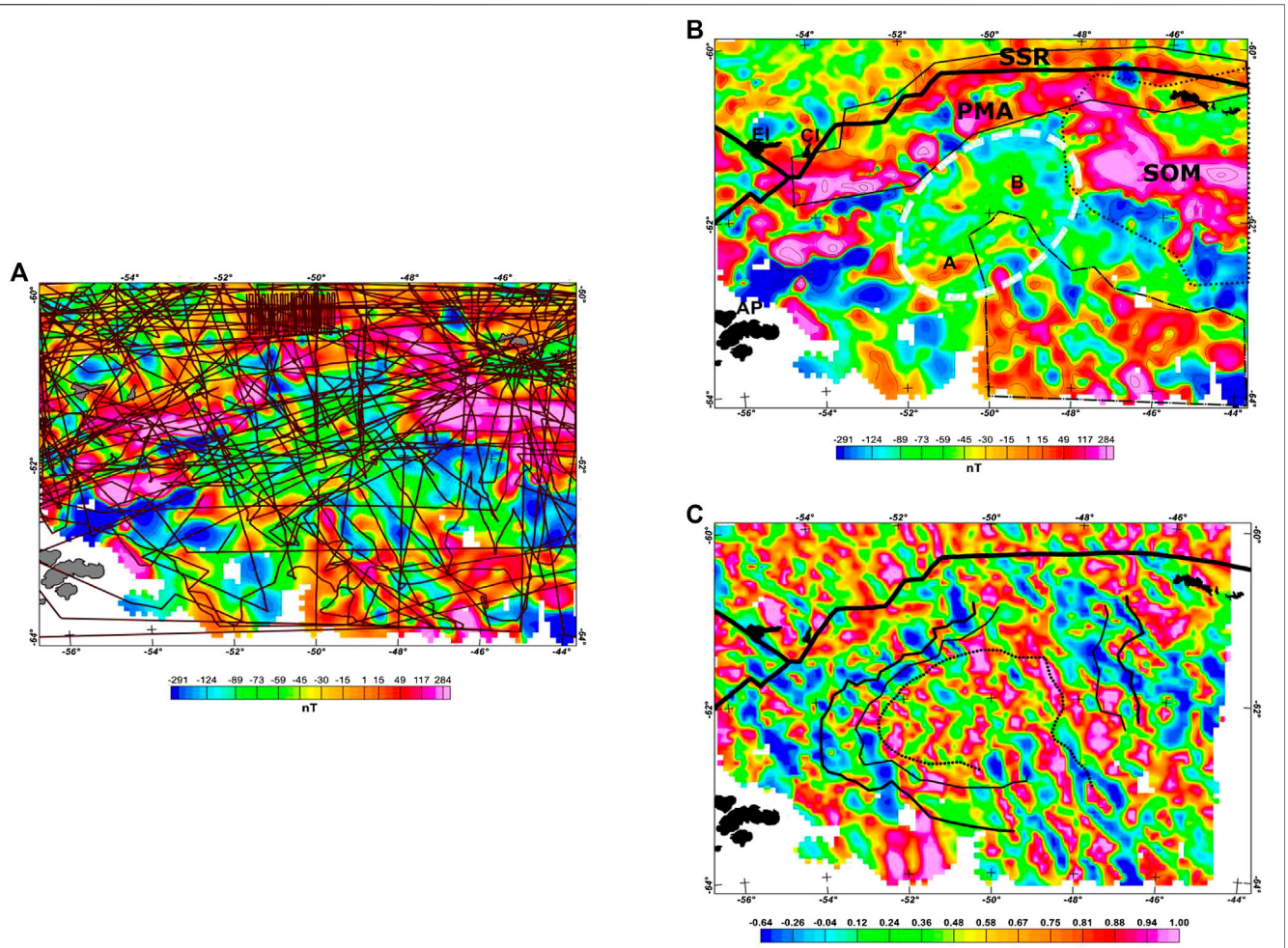

FIGURE 2 | A) Magnetic track line dataset of the study area. **(B)** Magnetic map of the area at 5 km resolution. Contour lines every 200 nT. Dotted, and dashed-dotted closed polygons highlight some features (see text for explanation). A thin solid black line surrounds the PMA. PMA, Pacific Margin Anomaly; SSR, South Scotia Ridge; SOM, South Orkney Microcontinent; CI, Clarence Island; EI, Elephant Island. Labels "A" and "B" mark the presence of two isolated magnetic anomalies. An elliptical white dotted outline marks Powell Basin's location. **(C)** A shaded relief map (illuminated from the NE) of the complete Magnetic anomaly map. Color palette represents non-dimensional surface reflectance coefficients. Thick and thin lines denote abrupt changes on the horizontal gradient magnitude applied on the TTS map (see text for details). A dotted line delimits the outer boundary of the oceanic area. Plate boundaries in black solid thick lines.

our result, more than those achieved by studies based in only one technique or method.

Additionally we aim to characterize and better understand the Powell Basin crustal and thermal structure and its relationship with the Scotia Sea asthenospheric flow, which deals with the transfer of asthenospheric material from the Pacific Ocean into the Atlantic (Martos et al., 2019). Overall, we analyze the role that this asthenospheric material could have played in the formation and state of the art of Powell Basin.

DATA AND METHODS

For this study, we used magnetic, gravity, sediment thickness derived from multichannel seismic and bathymetric data. Below we describe technical aspects related to the information used and method applied in our study.

Magnetic Data

We have used data from a compilation of marine magnetic anomalies, which served as a source for the second version of the World Digital Magnetic Anomaly Map (Quesnel et al., 2009) (**Figure 2A**). The data set uses the CM4 magnetic model to extract the core and external field contribution (Sabaka et al., 2004). It was cleaned by means of a careful check to increase its coherency. It means a track-by-track analysis of each data to correct or to remove many shifted values as well as to reduce the noise in some track lines. To reduce inconsistencies between neighboring lines, long-wavelength magnetic anomalies were adjusted using the NGDC-720 model, and line leveling. Besides these publicly available data, we used eight Spanish cruises carried out onboard the R/V Hespérides between 1992 and 2013. Finally, we obtained a magnetic anomaly map with 5 km resolution (**Figure 2B**) using a Kriging algorithm of interpolation (Cressie, 1990). This

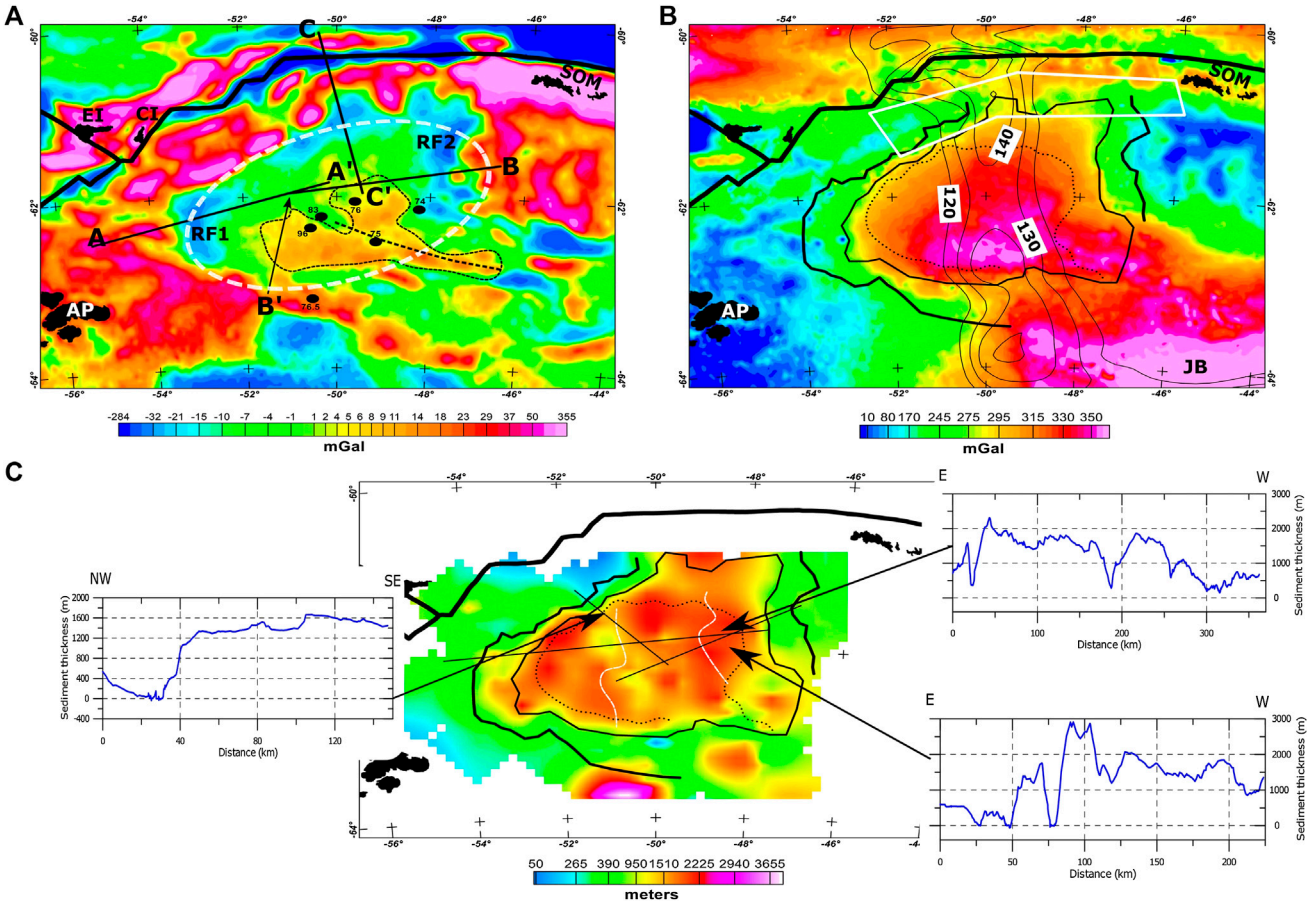

FIGURE 3 | A) Free-air gravity anomaly map. RF1 and RF2 denote two rift basins as in Eagles and Livermore (2002). Three black lines (A–A′, B–B′, and C–C′) mark location of three profiles plotted at **Figure 5**. A dotted polygon delimits a Y-like shaped high, which runs along the central part of the basin with a NW–SE trend. An elliptical white dotted outline marks Powell Basin's location. A dotted black line marks the extinct spreading axis. In black circles Heat flow values published by Lawver et al. (1994) in mW/m^2, **(B)** complete Bouguer gravity anomaly map. A white polygon highlights a gradient area. Three thin black contour lines denote HF isolines: 120, 130, and 140 mw/m^2. **(C)** Sediment thickness map of the study area. In white a line delimiting a low amplitude magnetic anomaly area (see text for explanation). Plate boundaries in black solid thick lines. Three original profiles show the variation of sediment thickness along the basin. AP, Antarctic Peninsula. EI, Elephant Island; CI, Clarence Island; SOM, South Orkney Microcontinent; JB, Jane Bank.

interpolation differs from simpler methods, such as Inverse Distance Weighted Interpolation, and Linear Regression among others, that it determines the most likely value at each grid node based on a statistical analysis of the entire data set. The Kriging interpolation method helps to avoid possible distortions caused by random data locations, when along-track and across-track density reading are unbalanced, or when the data acquisition lines have random directions (**Figure 2A**). We have illuminated the magnetic anomaly map from NE (**Figure 2C**). This map enhances the NW–SE trends while it severely attenuates the NE–SW trends.

Gravity and Bathymetry Data and Procedure

To characterize the study area, we have used the global free air dataset from Sandwell et al. (2014), with a resolution of 1 nautical mile (**Figure 3A**). To obtain the Bouguer gravity anomaly, water slab was corrected using a density of 1.03 g/cm^3. Complete Bouguer anomalies were calculated following Nettleton (1976) procedure. To control the bathymetry and to apply terrain corrections, we used the SRTM30plusv7 grid (1 km resolution). We used a subsampled version (10 km) of this grid as a regional grid to correct the gravity data beyond 10 km (Becker et al., 2009). We have used 2.67 g/cm^3 as terrain density. Finally, we obtained a Complete Bouguer anomaly grid with 2 km resolution (**Figure 3B**).

Sediment Thickness Data

We have used Multichannel Seismic (MCS) profiles at the Powell Basin and its surroundings extracted from the Seismic Data Library System. These profiles have been acquired within the framework of different projects carried out by several countries and with various acquisition systems including two obtained by the R/V Hesperides (HESANT 92/93 and SCAN97). More details about the profiles can be found at https://www.scar.org/data-databases/sdls/.

The seismic data acquired on board the R/V Hesperides (HESANT 92/93 and SCAN97) was processed on DISCO/FOCUS® software using standard procedures which include common depth point stack and time migration. The rest of

the profiles used for the basement identification were extracted from the Seismic Data Library System in stack version. The high data quality allows the visual identification of the basement across the Powell Basin and its margins. We interpreted the seismic profile in a KINDOM Suite® software base project, where the basement was identified and manually picked. The sediment thickness (**Figure 3C**) has been calculated taking into account the average velocities of the sedimentary layers proposed by King et al. (1997) using a seismic refraction experiment in Powell Basin. **Figure 3C** shows the distribution of the sediment layer. We have included three original profiles showing the variation of sediment thickness along the basin.

Total Tectonic Subsidence

Sawyer (1985) defined the term TTS as the difference between the pre-rifting continental crust elevation, and the present sediment-unloaded basement depth in a sedimentary basin. He used TTS as a tool to investigate the subsidence along profiles across the North American Atlantic margin in order to identify different types of crust at the US Atlantic margin, and to determine the location of the continent-ocean transition. This method assumes that continental crust was located at, or close to, sea level before rifting and subsidence took place.

This parameter has proven to be useful to study passive margin evolution through vertical movements on the basement. The TTS helps us to infer mechanisms of formation, or the processes that lead to deformations. It can be applied to multiple points in a basin and it is thus ideal for basinwide, or even continent-wide analysis. As it was pointed out before, it was used by Sawyer (1985) to identify different types of crust at the US Atlantic margin. Henning et al. (2004) used it at northern west Iberia margin along seismic lines. They calculated the thickness of oceanic crust, continental crust, and serpentinized mantle required to explain their observed TTS depths values along each line. Catalán et al. (2015) used the TTS together with potential field data analysis in a review about the state of knowledge in the Iberian Atlantic margin. They described and analyzed three provinces in this margin: the Galicia margin, the southern Iberian abyssal plain, and the Tagus abyssal plain. All this information was used to set limits for the continental crust domain, and the amplitude of the so-called ocean-continent transition zone.

As TTS represents the present, sediment-unloaded basement depth, it can be derived by just adding the water depth (H) and the sediment thickness (Z) plus the sediment loading effect.

It is important to note that the TTS describes where the basement surface is only due to tectonics. For that it is necessary to remove not only the sediment layer but also to eliminate too the sediment loading effect. Accordingly, the TTS value is obtained applying **Eq. 1**[1]

$$\mathrm{TTS} = H - Z + \mathrm{Isos\_Corr} \quad (1)$$

Sawyer (1985) discussed in detail two different models to calculate the loading responses of the lithosphere. The first ignore the flexural rigidity of the lithosphere while the second used a constant flexural rigidity for the crust. The TTS curve calculated ignoring the flexural rigidity was smoother than the TTS obtained with the second model (constant flexural rigidity). He interpreted that the first method removes equal amounts of short and long period variation of the sediment-loading signal, while the second method only removes the long-period component. Nevertheless he concluded that the TTS curves obtained through both different methods were similar, and the locations of major inflection points were the same. Sykes (1996) discussed different methods to infer the sediment loading correction or isostatic correction on oceanics domain depending on the sediment layer thickness. In our study MCS data show that sediment thickness ranges from 200 m on the borders to as thick as 2 km all along the basin (**Figure 3C**). Such a range of variation makes difficult to apply suitable algorithms, which do not introduce sharp gradients (artifacts) in the boundaries between thin and thick sediment layer areas.

Sykes (1996) proposed a second-order polynomial curve as the line of "best fit" to actual isostatic correction data. This equation assumes a uniform sediment density, irrespective of either water or depth or total sediment thickness. Sykes (1996) derived it using density-depth equations suitable for calcareous, clay and terrigenous sediment sequences. These hypotheses are acceptable in our study area (Barker et al., 1988). Sykes (1996) shows that it is accurate to within 60 m when compared to isostatic corrections calculated using ODP/DSDP data.

This correction has been applied by Heine et al. (2008) and Heine and Müller (2008) to get the TTS on intracontinental areas such as Arabian Basins, or in Eastern Australia to analyze anomalous tectonic subsidence.

For our study we have applied two procedures to eliminate the sediment loading effect: a) the first algorithm tested by Sawyer (1985), where flexural rigidity was ignored, and b) a simpler version of the algorithm proposed by Sykes (1996), as follows:

$$\mathrm{Isos\_Corr} = 0.43\,Z - 0.01\,Z^2 \quad (2)$$

We have applied both corrections in our study area and detected that although the specific TTS values obtained were not the same, we corroborate that the points where slope changes coincided. Accordingly the limits of the different domains were the same too.

To obtain the TTS map we created a geo-reference database with the available sediment thickness data at the study area. Using the sediment thickness data and **Eq. (2)** we calculated the sediment loading effect for every geographical location. In the same way we obtained the water depth using the SRTM30PLUS v7 grid. Using **Eq. (1)** we got the TTS. Finally we interpolated our TTS results at 5 nautical miles resolution (**Figure 4A**).

RESULTS

Magnetic Anomaly Map

The northern and western part of Powell Basin are characterized by large and long-wavelength positive magnetic anomalies (>300 nT) (**Figure 2B**). These anomalies correspond to the Pacific Margin Anomaly (PMA), which runs sub-parallel along the Antarctic Peninsula margin (Garrett, 1990; Ghidella et al.,

[1]Note that water depth is negative, while sediment thickness and isostatic correction are positives.

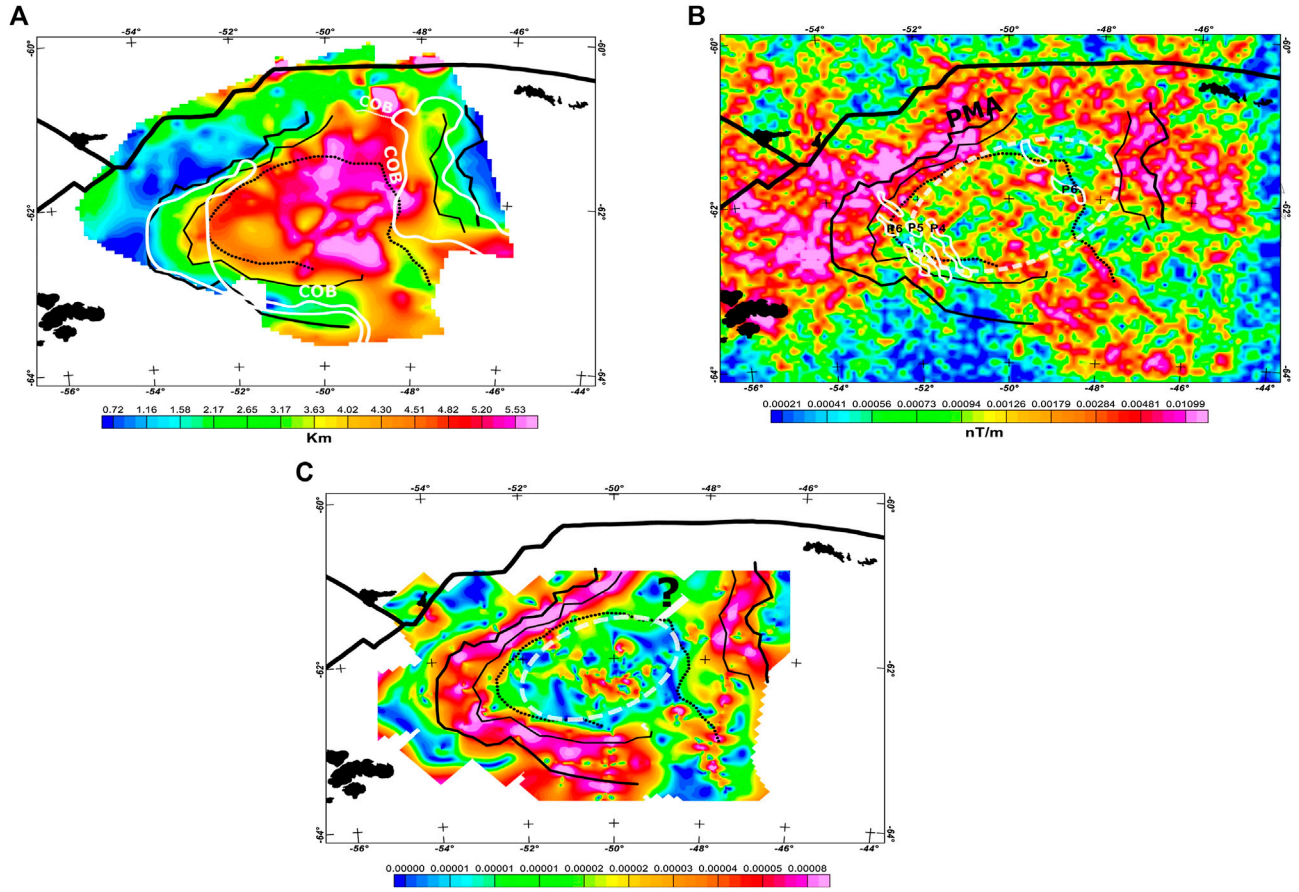

FIGURE 4 | A) TTS map. In white King et al. (1997)'s interpretation of several features as follows: A white solid curvilinear polygon in the East and West margins of Powell Basin depicts the location of areas interpreted as extended continental crust. The outer flanks of the previous cited curvilinear polygon was identified as continent-ocean boundary (COB labels in white mark its location). In thin white dotted line COB's interpreted location (northeastern part of the basin). **(B)** Analytical signal of the filtered magnetic map. An elliptical white dotted outline marks Powell Basin's location. In white solid lines some magnetic lineations (P4, P5 and P6) identified in Eagles and Livermore (2002). PMA, Pacific Margin Magnetic Anomaly. **(C)** TTS horizontal gradient map. Thick and thin black lines delimit abrupt changes on the horizontal gradient magnitude. A black dotted line delimits the outer boundary of the oceanic domain. Plate boundaries in black solid thick lines. A black question mark denotes an area whose continental nature is not concluded.

2002; Martos et al., 2014a). PMA extends without interruption until Bransfield Strait, where it is divided into two parts running north and south respectively. PMA anomaly has been subject of study by several authors (e.g., Garrett, 1990; Suriñach et al., 1997). It is considered a linear batholithic complex related to a Mesozoic–Cenozoic magmatic arc, which initially follows the whole Pacific–Antarctic margin, and locally split into two parts in the Bransfield Strait due to the expansion of this back-arc basin (Catalán et al., 2013). This anomaly extends along the SSR, and the SOM (**Figure 2**: inside solid and dotted polygons respectively). It was fractured during the opening of the Powell Basin at Oligocene times and the eastward drifting of the SOM. This fragmentation has continued during Cenozoic as a result of transtensional tectonics at the SSR (Suriñach et al., 1997; Bohoyo et al., 2007).

The southern east margin of Powell Basin includes a magnetic anomaly delimited by a dashed-dotted line in **Figure 2B**, which surrounds the SOM's southern margin toward the east. The central part of Powell Basin does not show large amplitude for the magnetic anomalies but several isolated ones (labeled as "A" and "B" in **Figure 2B**).

Several authors support the existence of oceanic crust in Powell Basin after a NE-SW spreading (King and Barker, 1988; Coren et al., 1997; Rodríguez-Fernández et al., 1997; Eagles and Livermore, 2002). Magnetic anomalies are key to support this possibility. As the amplitudes of the magnetic anomalies are small, we have enhanced a particular directional trending on the magnetic anomaly map (**Figure 2C**). It shows a similar picture to that used by Eagles and Livermore (2002) (their **Figure 3A**).

Free Air and Bouguer Gravity Anomaly Map

According to the free-air gravity anomaly map of the Powell Basin, free-air gravity anomaly amplitudes are moderate (between −30 and 40 mGal). A general high background characterizes the basin with two linear lows in its western and

northeastern margins (**Figure 3A**: RF1 and RF2, respectively). These two free-air gravity anomalies are considered as rift basin areas (Eagles and Livermore, 2002). A Y-like shaped high runs along the central part of the basin with a W–E and NW–SE trends (inside a dotted polygon in **Figure 3A**). A dotted black line marks the extinct spreading axis (Rodríguez-Fernández et al., 1997; Eagles and Livermore, 2002).

The Bouguer anomaly map shows a simple picture, where the highest values are located within the basin (280 mGal), related to oceanic crust, being surrounded by low amplitudes (<80 mGal) related to the Antarctic Peninsula and the South Shetland Archipelago (to the west), and SOM (to the east) (**Figure 3B**). These low amplitude anomalies are disrupted in the northern part of the basin. The gravity high in the central part of the basin extends linearly to the southeast, where it connects with an E–W positive trend anomaly corresponding to the Jane Bank (**Figure 3B**).

Figure 3B (inside a white polygon) shows in the north the presence of a gravity gradient zone where Bouguer gravity anomaly values change from low to high values from the west to the east reaching again low amplitudes at the SOM. We interpret this as thinned continental blocks, relict of the break up of the Antarctic Peninsula block, which finally led to the shift of SOM to its current position in the upper Miocene.

Identification of the Ocean-Continent Transition Zone. The Continent Ocean Boundary

Continental rifting involves a combination of tectonic and magmatic processes. Rifting is not a continuous process, and the amount of extension varies along time. These changes in extensional regimes appear in the TTS slope. The use of horizontal derivatives on the TTS grid is sensitive to changes in the TTS slope, and helps delineating the different extensional pulses occurred throughout rifting, while using the Analytic signal helps delineating the boundary where oceanic domain begin as this operator will maximize the contrast of magnetization.

Analytic Signal

After obtaining the magnetic anomaly map, we calculated the analytic signal (AS). This is defined as the square root of the squared sum of the vertical and two orthogonal horizontal derivatives of the magnetic field anomaly (Roest et al., 1992; Roest and Pilkington, 1993; Salem et al., 2002).

$$\left|\mathrm{AS}(x,y,z)\right| = \sqrt{\left(\frac{\partial M}{\partial x}\right)^2 + \left(\frac{\partial M}{\partial y}\right)^2 + \left(\frac{\partial M}{\partial z}\right)^2} \qquad (3)$$

where $\left|\mathrm{AS}(x,y,z)\right|$ is the amplitude of the AS, and M is the magnetic anomaly intensity.

Therefore, the resulting 3D-AS map summarizes the net variation of the gradient of the magnetic anomaly field intensity in 3D. One of the most attractive aspects of this 3D operator is the fact that its amplitude produces highs over magnetic contacts regardless of the direction of magnetization or its induced and/or remnant character (Roest et al., 1992; Roest and Pilkington, 1993; Keating and Sailhac, 2004). In this sense, there is no need to assume a purely induced magnetization effect or to discuss possible remnant vector space orientation. This simplistic approach (a purely induced magnetization effect hypothesis) could lead to distortion in environments where remnant effects are high. This operator highlights horizontal magnetization contrast and helps to delineate the oceanic domain boundary.

As the PMA saturated the AS color map, we used a directional filter, which highlights NW–SE trending on the magnetic map (cut-off wavelength is 20 km). Then the AS was obtained using this filtered map. **Figure 4B** shows the result.

Total Tectonic Subsidence Horizontal Gradient

Going deeper into the TTS analysis and in order to locate abrupt changes in the TTS signal, we obtained the horizontal gradient of the TTS map using the two orthogonal horizontal, x and y, derivatives as follows:

$$\mathrm{HG}(x,y) = \sqrt{\left(\frac{\partial M}{\partial x}\right)^2 + \left(\frac{\partial M}{\partial y}\right)^2} \qquad (4)$$

where M represents the TTS, and HG the value of its horizontal gradient.

This procedure resembles the technique proposed by Blakely (1995) and Grauch and Cordell (1987). They show that highs in the horizontal gradient reflect the edges of gravity sources (Blakely, 1995). It allows us to detect important lithospheric boundaries.

The methodology we have followed consists of obtaining the horizontal gradient of the TTS, and contouring the horizontal gradient magnitude on the map. **Figure 4C** shows the results obtained. The highest TTS gradient values surrounding Powell Basin are displayed and delimit between a thick and a thin black line. Another boundary is shown in the same figure between the thin and dotted black line. Both areas constitute what we will refer as OCTZ.

Lithospheric Boundary Interpretation

We use a combination of techniques and data including TTS, Bouguer gravity anomaly, and Analytical signal to study the nature of the crust in three different margins at Powell Basin. To accomplish this we have selected three different profiles (see **Figure 3A** for geographic location): profile A–A′ with a WSW–ENE trend in the western margin (**Figure 5A**), profile B–B′ with a W–E trend in the eastern margin (**Figure 5B**), and profile C–C′ with an N–S orientation in the northern margin (**Figure 5C**).

Western Margin (Profile A–A′)

In the selected profile that characterizes the western margin of the Powell Basin, A–A′ (**Figure 5A**), we distinguish three linear trends in the TTS signal: a first zone which goes from 70 to 123 km (background Pattern-horizontal lines), a second zone

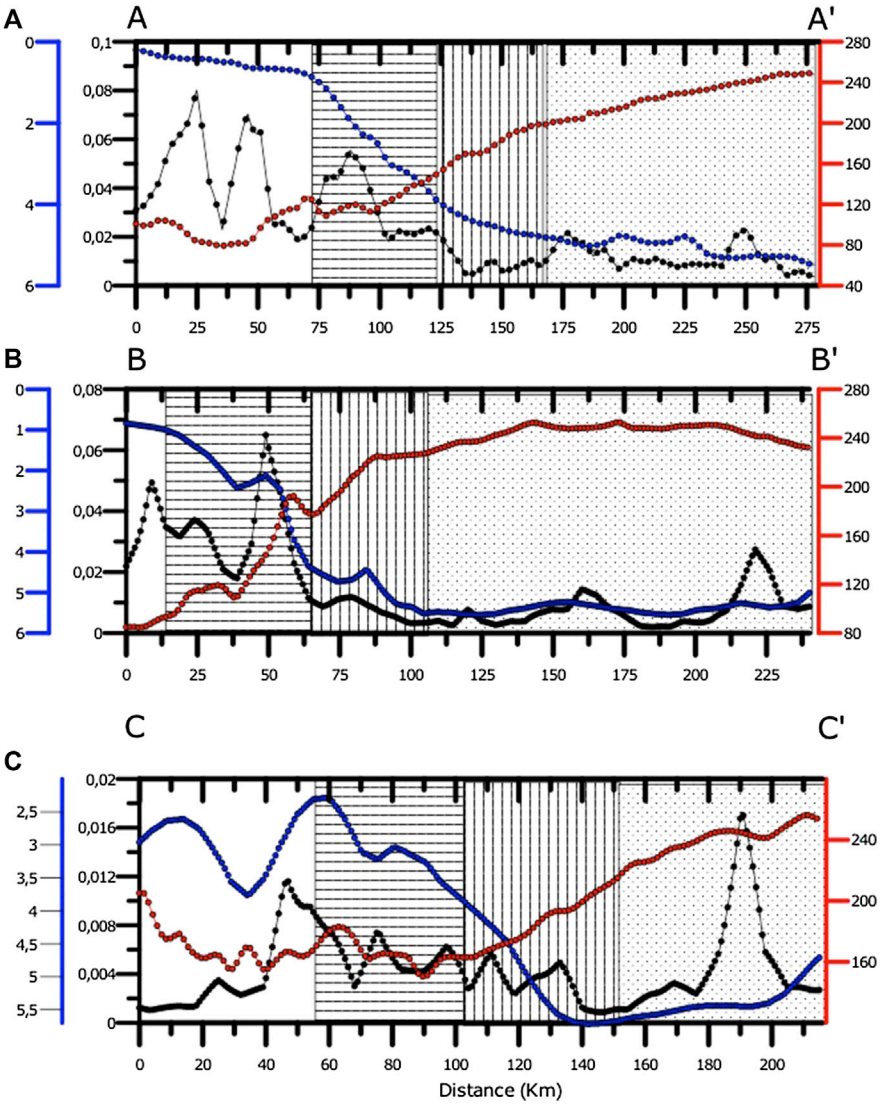

FIGURE 5 | Analysis of three profiles [see **Figure 3(A)** for profiles location]. **(A)** Western margin, **(B)** eastern margin, and **(C)** northern margin. In blue: TTS in kilometres. In red: Bouguer gravity anomaly in mGal. In black: Analytical signal in nT/m. Zone using horizontal, vertical or dotted lines as background denote different tectonic domains (see text for clarification).

which goes from 123 to 166 km (background Pattern-vertical lines), and a third segment which starts at 166 km until the end of the profile (background Pattern-dotted). The highest slope in TTS profile is located between 70 and 123 km. The AS signature shows large amplitudes and variations from the beginning of the profile and into the first zone. This corresponds to the PMA. The Bouguer gravity anomaly values increase monotonically from 111 to 148 mGal, which corresponds to a thinned continental crust. Between 123 and 166 km, the rate of increase of Bouguer gravity anomaly is lower than at the first zone. The AS signature shows a clear change of style, which is kept throughout the rest of the profile. The TTS shows an almost flat signal from 130 km onwards that we interpret as a continental intruded crust with magmatic material (hereafter continental intruded crust). From 166 km until the end of the profile, we find that the Bouguer gravity anomaly values larger than 200 mGal. The TTS is flat. Altogether, and the NW–SE trending magnetic anomalies identified in this area (**Figure 2C**) suggests an oceanic nature in this domain.

Eastern Margin (Profile B–B′)

From **Figure 5B** we also distinguish three linear trends in the TTS: a first zone which goes from 12 to 63 km (background Pattern-horizontal lines), a second zone which goes from 63 to 104 km (background Pattern-vertical lines), and a third segment which started at 104 km until the end of the profile (background Pattern-dotted). The sharpest slope in TTS profile is located between 12 and 63 km. Bouguer gravity anomaly values increase monotonically from 95 to 191 mGal. Along this first zone the AS shows large values corresponding to the SOM. We

interpret this area as a thinned continental crust. Between 63 and 104 km, the rate of increase of Bouguer gravity anomaly is lower than between 12 and 63 km, while the TTS keeps on decreasing at a lower rate. The AS shows a clear change of style. We interpret this zone as a transitional continental thinning area. From 104 km until the end of the profile, the TTS reaches almost flat. The AS shows on average low values but periodic fluctuations, which we attribute to oceanic spreading anomalies. Bouguer gravity anomaly values are larger than 230 mGal. Based on the above and the NW-SE trending magnetic anomalies identified in the area (**Figure 2C**) this is considered as an oceanic domain.

Northern Margin (Profile C–C′)

From **Figure 5C** we distinguish three linear trends: a first zone which goes from 58 to 103 km (background Pattern-horizontal lines), a second zone which goes from 103 to 151 km (background Pattern-vertical lines), and a third segment which started at 151 km until the end of the profile (background Pattern-dotted). We interpret the first zone as a thinned continental crust, the second zone as transitional continental thinning area, and the third as an oceanic domain. The large AS peak at km 190 is associated with a local feature (**Figure 2B**: magnetic anomaly label as "B"). The Bouguer gravity anomaly profile shows a smoother transition compare with TTS, reaching stable values almost 50 km ahead. This makes a difference with the previous profiles [western (A–A′) and eastern (B-B′)] as Bouguer gravity anomaly profiles roughly behave as a specular image of TTS (**Figures 5A,B**).

DISCUSSION

We performed an integrated study on Powell Basin using gravity, magnetics and TTS data. In this section we will firstly discuss the tectonic boundaries. To achieve this we extrapolate to a 3D our previous 2D results using the TTS, Bouguer gravity anomaly, and Analytical signal information altogether to discuss the nature of the crust in three different margins of Powell Basin. Additionally, we compare our results with other proposals for tectonic domains (King et al., 1997), or oceanic domain extension (Eagles and Livermore, 2002). Finally, we analyzed the low amplitude of its magnetic anomalies and shed some light on this unresolved issue to date. We point to the possibility that a heat injection of the Pacific mantle outflow trough one astenospheric branch can explain it.

Determination of the Different Tectonic Boundaries

Figure 4C shows the TTS horizontal gradient. The outer limits of the largest TTS gradient values surrounding Powell Basin are displayed as a thick line. Other remarkable boundaries are shown as a thin line or as a dotted line. To interpret these areas we checked the profiles shown in **Figure 5**. The highest gradient's area is broad and immediately follows the continental area. Roughly speaking it coincides with the area with horizontal lines as background pattern. We interpret it as an extended continental crust. The other boundary (**Figure 4C**: between the thin and dotted black line) immediately follows it. It represents a smoother transition coinciding with the zone with vertical lines as background pattern (**Figures 5A–C**). Both areas (between the thick and thin lines, and between the thin and dotted line zones) contain large magnetic anomalies, and a similar AS signature (**Figure 4B**). Particularly, the area between the thin solid and dotted black line holds a lower slope values in the TTS. We interpret the area, as extended and intruded continental crust. Both areas: the extended continental crust and the extended and intruded continental crust conform the OCTZ according with our interpretation. As we get into the basin, the AS amplitudes and signature change sharply. A predominant NW-SE trend can be depicted. As it was pointed out, the smallest slope in the TTS fall within this area. We interpret this zone as an oceanic domain.

Figure 6 represents our sketch map of inferred tectonic boundaries at Powell Basin. King et al. (1997) provided a sketch map of the significant tectonic elements of Powell Basin and proposed a tentative location of the COB as well as the location of extended continental crust based on seismic profiles (see **Figure 4A** curvilinear polygon in white lines and **Figure 6** in blue). It is worth noting that they only recognize one area, which they interpreted as an extended continental crust.

There is a good agreement between our proposal and their results. Nevertheless, the uses of horizontal gradient and AS plots allow us to recognize the existence of an intermediate area where not only extended but also intruded continental crust exists. Throughout the whole western margin, the area interpreted in this study as extended crust (between thick solid and thin solid lines), and the area interpreted in this study as extended and intruded continental crust (between thin solid and dotted lines) have a roughly constant width.

King et al. (1997) recognize only one area. They interpreted it as an extended continental crust. In their interpretation (**Figure 4A**, white solid lines) this zone presents a large development in the central western zone (approx. 76 km), while its width decreases to below 20 km in the southwestern zone. According with our results the OCTZ shows a similar width in the southwestern area than in the central western zone. We attribute this difference to the fact that we use magnetism (through AS), which helps to better constrain the COB, and the limit between extended continental crust and extended and intruded continental crust. Besides the greatest difference in seismic coverage between our study and King et al. (1997) occurs precisely in this area where our coverage is better.

Regarding the nature of the area located in the north-eastern sector and out of our proposal for an oceanic domain, we cannot conclude if it is a continental intruded crust or purely extended continental crust. At the south-eastern sector, the COB is not well constrained from the TTS map, as the seismic coverage is coarse. Nevertheless, the AS map delimits quite well a magnetization contrast which we interpret as the COB (**Figure 4B**).

The oceanic crust province in Powell Basin is smaller as defined in this paper in relation to the one defined by Eagles and Livermore (2002) and King et al. (1997). Eagles and Livermore (2002) interpretation for the set of magnetic anomalies (their **Figure 3B**) shows magnetic anomaly P6 (western side) inside the extended and intruded continental

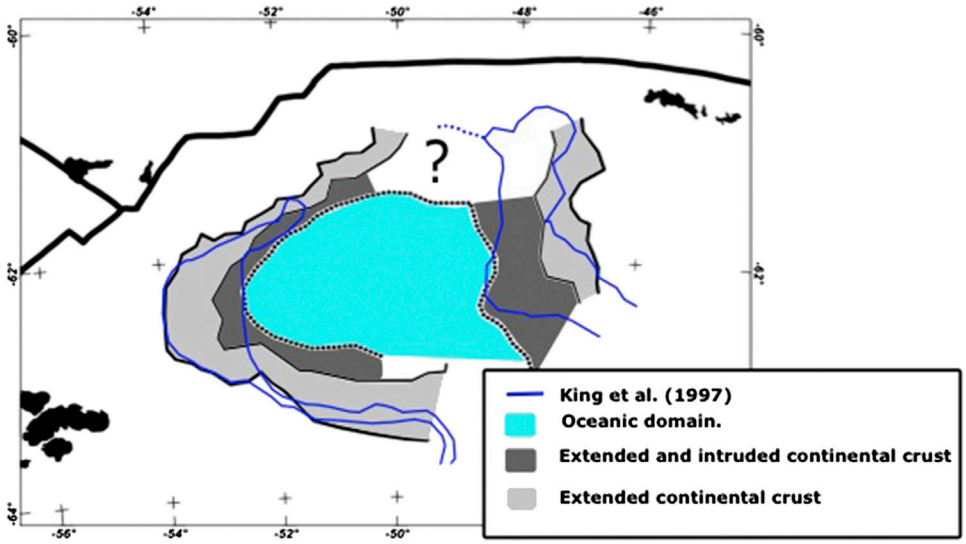

FIGURE 6 | Sketch map of the different tectonic domains in Powell Basin. In light gray and in dark gray areas we interpret as extended continental crust, and as extended and intruded crust, respectively. In light blue: oceanic domain. A blue solid curvilinear polygon in the East and West margins of Powell Basin depicts the location of areas interpreted as extended continental crust by King et al. (1997). In the East and West margins King et al. (1997) identified the outer flanks of the previous cited blue curvilinear polygon as COB. Location of the COB (according with King et al. 1997) in the northeastern part of the basin in thin black dotted line. A black question mark denotes an area whose continental nature is not concluded.

area. Moreover, **Figure 2C** shows linear magnetic anomalies, and some are included in the transitional area (continental intruded crust). We interpret them as magmatic material intruded in fractures. These fractures present an NW-SE orientation and produce linear magnetic anomalies, which cannot be interpreted as oceanic magnetic anomalies due to seafloor spreading but due to intrusion and later cooling of magmatic material. These magnetic anomalies were investigated offshore west Iberia by Russell and Whitmarsh (2003), and Sibuet et al. (2004). They attributed those magnetic anomalies as indicative of a highly extended continental crust rather than the upper layer of a standard oceanic crust.

Abnormal Low Amplitude of Powell Basin's Magnetic Anomalies

Several authors (e.g., King et al., 1997; Eagles and Livermore, 2002) highlighted the presence of low amplitude magnetic anomalies in Powell basin (40 nT peak to peak). Levi and Riddihough (1986) proposed that magnetic anomalies could be suppressed as a result of pervasive hydrothermal reactions underneath the sediment layer. In this way, the sediment layer created a closed hydrothermal system by preventing fluids venting directly into the overlying cold seawater. This retention of hot fluids would have caused leaching of iron oxides, reducing the amplitude of magnetic anomalies. King et al. (1997) proposed this reason to justify the absence of clear seafloor magnetic anomalies at Powell Basin. As already indicated in the introduction, although the proposed models by Coren et al. (1997) and Eagles and Livermore (2002) consider the basin's creation between the Oligocene and the Upper Miocene, the small amplitude of these anomalies makes it difficult to determine the age of the basin unequivocally.

In order to isolate and detect seafloor spreading magnetic anomalies in Powell basin to understand the nature of the basin as well as geodynamic processes in the area, we have applied a high-pass filter using a 50 km cut-off wavelength to disregard regional trends (**Figure 7**). In addition, we also selected profiles that run across the basin (**Figure 8**) to quantify the amplitude of the magnetic anomalies. Similar procedure was performed by Eagles and Livermore (2002), when they used an isotropic bandpass filter, passing wavelengths between 30 and 50 km, with taper to 75 and 1 km with the addition of a directional cosine filter to enhance the N30°W orientation. The high-pass filtered map (**Figure 7**) and the selected profiles (**Figure 8**) help us to describe the location of high concentration of low amplitude magnetic anomalies. The profiles show amplitudes ranging below 40 nT peak to peak, reaching values higher than 100 nT in some areas (i.e., eastern area at middle profile). These large values are due to local features and are located in a thinned or transitional continental zone. The three profiles at **Figure 8** shows an area (delimited by a gray filled square) where the magnetic anomaly amplitude decreases and oscillates between 20 nT peak to peak (profiles located in the north and in the central area), or between 10 nT peak to peak (southern and central profiles). In summary, there is an area where the amplitudes decrease approximately by a half with respect to those values achieved along the rest of the profile (**Figures 7** and **8**). A thick brown line delimits this area in **Figure 7**.

The sensitivity of magnetic properties with temperature seems to be key on understanding the existence of the abnormal low amplitude magnetic anomalies in Powell Basin concentrated in a

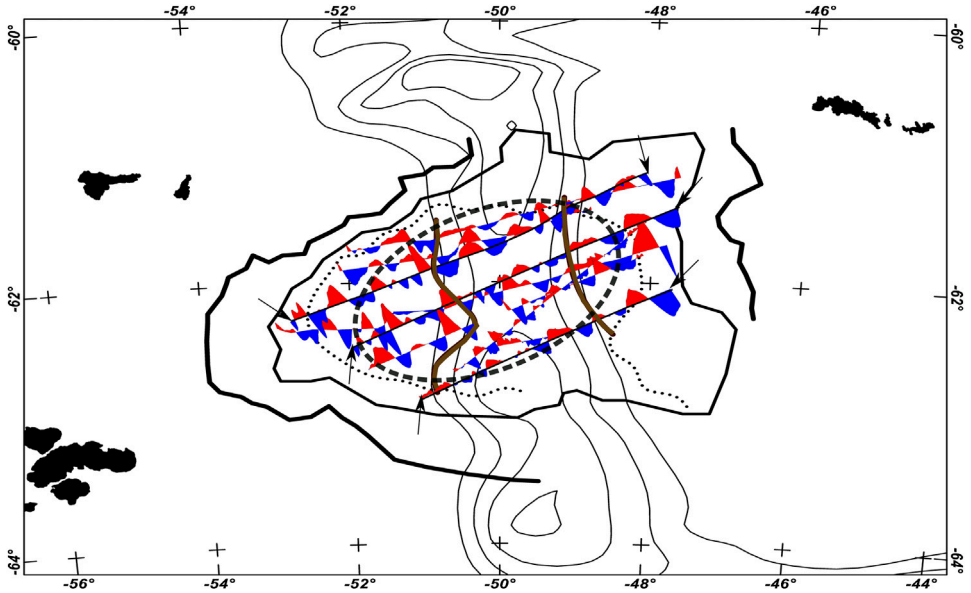

FIGURE 7 | Wiggle plot map showing some magnetic anomaly profiles along Powell Basin. Thin black contour lines denote HF isolines: 120, 130, and 140 mW/m^2 as in **Figure 3B**. A thick brown line delimits a low amplitude magnetic anomaly area. Three baselines corresponding with three magnetic profiles displayed in **Figure 8** are highlighted in black and their limits marked with arrows. An elliptical black dotted outline approximately marks Powell Basin's location. Thick and thin black lines delimit abrupt changes on the horizontal gradient magnitude. A black dotted line delimits the outer boundary of the oceanic domain.

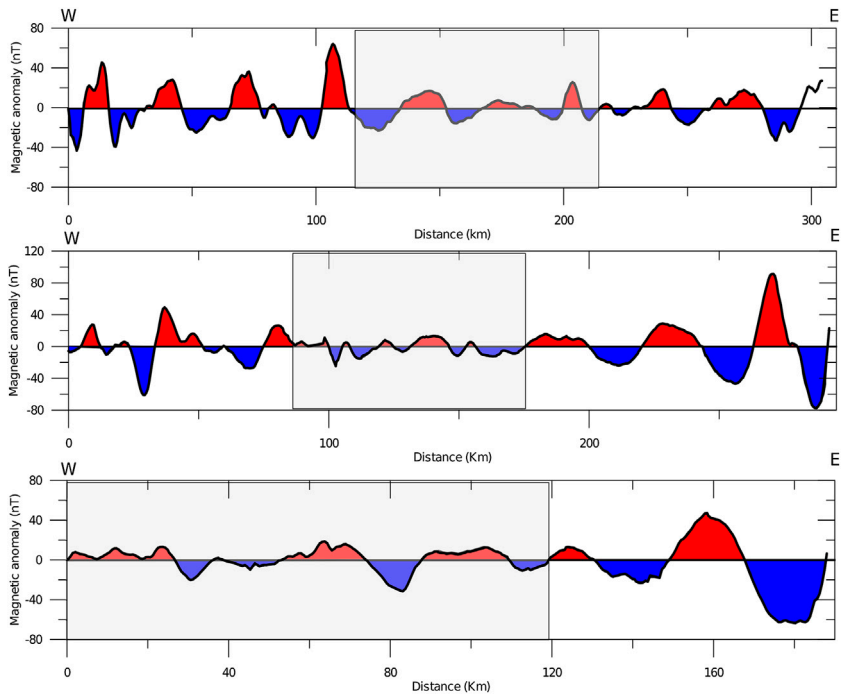

FIGURE 8 | Three magnetic anomaly profiles from Powell Basin. E, East; W, West. A gray filled square delimited an area where the magnetic anomaly amplitude abnormally decreases.

limited region. Studies by Martos et al. (2014b) and Martos et al. (2019) addressed an anomalous thermal regime of the lithosphere in the region.

Martos et al. (2014b) proposed the existence of an asthenospheric flow transfer from the Pacific into the Atlantic in which the Shackleton Fracture Zone and other major lithospheric blocks play a relevant role. This fracture zone would have been established along the middle Miocene (Martos et al., 2013) by acting its lithospheric roots as a barrier for the asthenospheric flows (Martos et al., 2014b). It would have divided the asthenospheric flow into two branches. One would run along the North Scotia Ridge, and the second along the south-western side of the Scotia Sea. The southern branch circulates along the northern margin of continental crust blocks scattered along the southwest of the Scotia Sea, deflecting toward the Weddell Sea (Martos et al., 2014b).

Martos et al. (2019) provided a map of geothermal heat flow (HF) of the Scotia Arc. This map has been obtained from magnetic anomaly data after applying spectral procedures. The aforementioned map shows the presence of high HF distributed along the Scotia Arc. This distribution has been interpreted in terms of asthenospheric currents. One of the branches runs north of the South Shetland Archipelago and enters into the Weddell Sea through the north of the Powell Basin. This asthenospheric current would have been established after the formation of the Shackleton Fracture Zone (middle to upper Miocene) (Livermore et al., 2004; Martos et al., 2013). According to that, this asthenospheric current system would have entered into the Powell Basin after its completion in the upper Miocene. If this were the case, a gravity signal must indicate this process in Powell Basin. For this, we analyze the Bouguer gravity anomaly map (**Figure 3B**). It shows a high gradient region at the north of the basin with values changing from low to high from the west to the east reaching again low amplitudes at the SOM (within the white polygon in **Figure 3B**).

The separation of the SOM from the Antarctic Peninsula block could have originated an area of lithospheric weakening which could have facilitated the access of a branch of asthenospheric current during the upper Miocene or during the Pliocene when the Scotia Arc regime changed to a left lateral movement and the South Scotia Ridge suffered a new extensional phase with the development of several pull-apart basins (Galindo-Zaldívar et al., 1996). The presence of this asthenospheric current likely contributed mantellic material through the north of the basin, which can justify such smooth variation of Bouguer gravity anomaly profile shown in **Figure 5C** while TTS profile evolved faster.

A reasonable correlation of the Bouguer gravity anomaly high area (high within the white polygon in **Figure 3B**) exists with the high geothermal heat flow determined by Martos et al. (2019). We have plotted the HF isolines from Martos et al. (2019) corresponding to 120, 130, and 140 mW/m^2 to prove this spatial correlation (**Figures 3B** and **9**). We also observe a good agreement of the region represented by low magnetic anomalies amplitudes (brown thick lines used at **Figure 7**) and the HF signal.

It could be argued that a 2–3 km sediment thickness layer could cause, at least to some extent, the attenuation that locally affects the amplitude of the magnetic anomalies. According to our results about the distribution of the sediment layer (**Figure 3C**), it does not seem reasonable to attribute the decrease in amplitude to a derived effect caused by the departure from the source produced by sediment layer as Powell basin presents an average thickness of 2 km.

Lawver et al. (1994) performed six heat flow measurements (**Figures 3A**, **9**). Generally speaking those values oscillates between 74 and 83 mW/m^2. The highest value (96 mW/m^2) is reported to be located in a basement high that they suggested it may be the extinct spreading center. In view of the free air gravity anomaly map (**Figure 3A**) this value falls not on the extinct spreading center but on one of the flanks of the Y-like shape high. According with this **Figure 3A** the values of 83, and 75 mW/m^2 would be located on this high. Martos et al. (2019) provided a map that show higher values in the same area (ranging from 120 to 140 mW/m^2). The difference between the measured Lawver et al., 1994) and estimated values (Martos et al., 2019) is due to the following reasons: a) Martos et al. (2019) provided average heat flow values of an area. They were obtained by applying spectral techniques on windows of 50% overlapping 250 × 250 km windows, while the values obtained by Lawver et al. (1994) represent local measurements only representative of the point where the measurement was taken. b) Lawver et al.'s (1994) readings lack sedimentation correction. Its application would provide higher values at all points and therefore they become more similar to those provided by Martos et al. (2019). c) The HF values provided by Martos et al. (2019) are estimations based on a conductive heat transfer mechanism, however, in the area near the ridge, hydrothermal circulation might be remarkable and therefore it is likely that heat is distributed in different ways than conduction. It might have affected local readings. Accordingly we believe that Martos et al. (2019) are a more reliable depiction of the regional variability of heatflow variability due to temperatures in the upper crust.

To understand the reason of the difference of magnetic anomaly amplitudes within Powell Basin we must analyze the magnetic structure of an oceanic crust. In general terms it is well stated that there are two magnetic layers. The first composed of extrusive basalts, where its main component is Titanomagnetite. Its thickness is less than 1 km. The second layer is composed of gabbros, dolerites and in some cases serpentinized peridotites. Its thickness is approximately 5 km (Choe and Dyment, 2019). Both contribute to the magnetic response but only the most superficial layer is responsible of the seafloor spreading anomalies (Tivey and Johnson, 1993; Schouten et al., 1999). The Curie temperatures are different: between 100–550°C for Titanomagnetite depending on the content of Ti and the degree of oxidation (Zhou et al., 2001), and 580°C for magnetite, which is the most abundant magnetic component in the deeper layer (Choe and Dyment, 2019).

There are two factors that can alter the magnetic response of an oceanic crust: hydrothermal alteration and heat. Although hydrothermal alteration can affect magnetization, estimating its effect is hard to quantify. Particularly regarding our study area, it

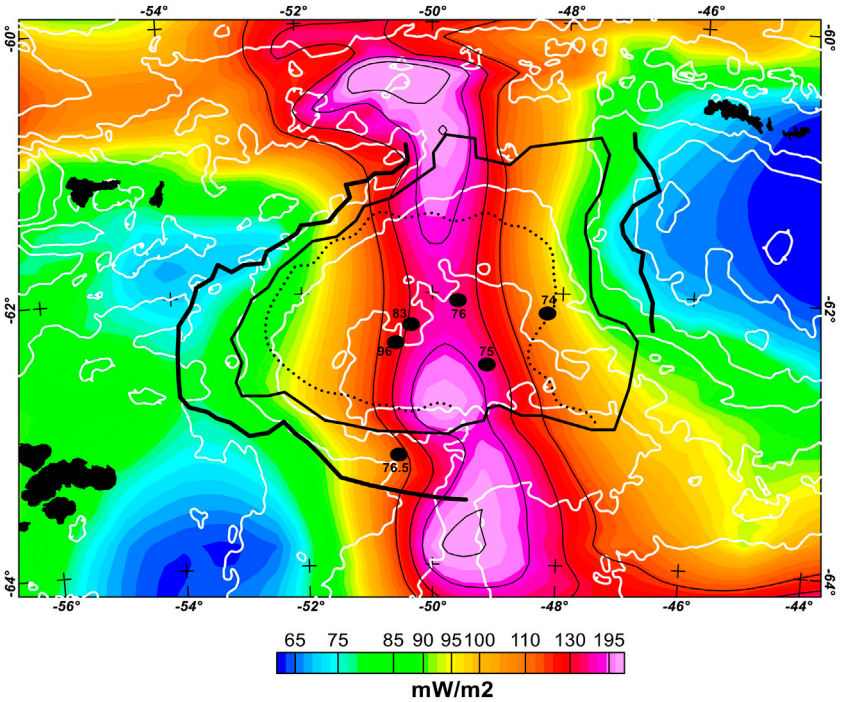

FIGURE 9 | HF map derived from magnetic data (see Martos et al., 2019 for details). Thin black contour lines denote HF isolines: 120, 130, and 140 mW/m^2 as in **Figure 3B**. Bouguer gravity anomaly contour lines in thick white color. Heat flow values published by Lawver et al. (1994) in mW/m^2.

is difficult to understand why the amplitudes of magnetic anomalies are smaller in a zone than in nearby areas with a similar sediment thickness. This leads us to think on some physical process that can affect in a greater extent that area, such as the asthenospheric current.

To estimate the temperature range between 2 and 3 km, which is the range of depths occupied by the extrusive basalt layer, we will use the heat flow values of Martos et al. (2019) and we will assume the following approximations: a) a purely conductive heat transfer model, b) an average thickness of 2 km for the sediment layer, c) an average value for the thermal conductivity of 3.138 W/mK for the lithosphere, which was the one used at Martos et al. (2019). All these assumptions lead us to estimate that temperature ranges 90–134°C between 2 and 3 km depth (bsf) in the central zone of the basin, while in the rest of the basin, the temperature ranges would be 60–91°C in the same depth interval.

This estimation suggests that the lowest Curie temperature for Titanomagnetite (100°C) is reached by the 76% of the extrusive basalt layer in the central zone, while it is never reached outside of it. This estimation fits with a smaller magnetization in the central area of the basin compared with the rest of the basin.

After analyzing gravity, magnetic, sediment thickness, and heat flow data, we propose that the asthenospheric supply from the Scotia Sea had a major impact into the evolution of Powell basin. The extra heat source from the asthenospheric branch likely decreased the total magnetization or the magnetic crustal thickness in the area, reducing the amplitude of the oceanic spreading magnetic anomalies in its central area. A similar scenario is found at Venezuela Basin (Caribbean Basin) where the presence of a high HF and a shallow Curie isotherm justify the absence of magnetic stripes in the area (Ghosh et al., 1984; Orihuela et al., 2013).

CONCLUSIONS

Using magnetic, gravity, bathymetry and seismic data, and applying mathematical operators such as total horizontal gradient and analytical signal, we have defined the boundaries of the different tectonic regions, which characterized Powell Basin: Extended and thinned continental crust, intruded and thinned continental crust, and oceanic domain. According to our results, the oceanic seafloor extension seems to be smaller than what was previously supported and our conclusions would affect future works constraining the age of the basin. This procedure can be applied in any basin or margin to define boundaries. In addition, we have detected the existence of an area where magnetic anomaly amplitudes are smaller (by almost a half) than in the rest of the basin. From the analysis of a Bouguer gravity profile vs. a TTS profile in the northern part of the basin, we have detected an abnormal behavior, which can be justified by the injection of high-density material from the SSR into the Powell Basin. The existence of a spatial correlation between this high-density channel, an HF branch coming from the Scotia Plate, and the area where magnetic anomaly values are almost systematically smaller than in the rest of the basin, lead us to support the role that the heat injection of the Pacific mantle outflow had in the basin's magnetic anomaly signature.

DATA AVAILABILITY STATEMENT

Publicly available datasets were analyzed in this study. These data can be found here: For marine magnetic data at https://www.ngdc.noaa.gov/mgg/. For multichannel seismic profiles at https://www.scar.org/data-databases/sdls/. For Curie Depth and Geothermal Heat Flow at https://doi.org/10.1594/PANGAEA.905428. For bathymetry at https://topex.ucsd.edu/WWW_html/srtm30_plus.html. For free air gravity data at https://topex.ucsd.edu/WWW_html/mar_grav.html.

AUTHOR CONTRIBUTIONS

MC and YM drafted the manuscript, and process the magnetic and gravity data. JG, FB, and LP compiled, and selected sediment thickness data from the Seismic Data Library System, and obtained the Total Tectonic subsidence data. FB contributed to improve the manuscript. All authors read and approved the final manuscript.

FUNDING

This study has been funded through project RTI 2018–099615-B-100 entitled "Estructura Litosférica y Geodinámica de Powell-Drake-Bransfield Rift" under the umbrella of the Programa Estatal de I + D + i Orientada a los Retos de la Sociedad of the Spanish Ministry of Science. JG, FB, and LP participation has been funded through project CTM 2017–89711-C2-2-P entitled "Timing and main tectonic processes involved in the onset and evolution of the Antarctic Circumpolar Current (ACC): development of continental margins and oceanic basins" under the umbrella of the Programa Estatal de I + D + i of the Spanish Ministry of Science.

REFERENCES

Barker, P. F., Kennett, J. P., O'Connell, S., Berkowitz, S., Bryant, W. R., Burckle, L. H., et al. (1988). *Proceedings of the Ocean Drilling Program, initial reports, vol. 113. Weddell Sea, Antarctica. Covering leg 113 of the cruises of the drilling vessel JOIDES Resolution, Valparaiso, Chile, to East Cove, Falkland Islands, Sites 689-697, 25 December 1986 - 11 March 1987*. College Station, TX: Ocean Drilling Program, 785. (Proceedings of the Ocean Drilling Program, 113).

Becker, J. J., Sandwell, D. T., Smith, W. H. F., Braud, J., Binder, B., Depner, J., et al. (2009). Global bathymetry and elevation data at 30 arc seconds resolution: SRTM30_PLUS. *Mar. Geodes.* 32 (4), 355–371. doi:10.1080/01490410903297766

Blakely, R. J. (1995). *Potential theory in gravity and magnetic applications*. New York, NY: Cambridge University Press.

Bohoyo, F., Galindo-Zaldívar, J., Jabaloy, A., Maldonado, A., Rodríguez-Fernández, J., Schreider, A., et al. (2007). Extensional deformation and development of deep basins associated with the sinistral transcurrent fault zone of the Scotia-Antarctic plate boundary. *Geol. Soc. Spec. Publ.* 290, 203–217. doi:10.1144/sp290.6

Bohoyo, F., Galindo-Zaldívar, J., Maldonado, A., Schreider, A. A., and Suriñach, E. (2002). Basin development subsequent to ridge-trench collision: the Jane basin, Antarctica. *Mar. Geophys. Res.* 23, 413–421. doi:10.1023/b:mari.0000018194.18098.0d

Catalán, M., Galindo-Zaldívar, J., Davila, J. M., Martos, Y. M., Maldonado, A., Gambôa, L., et al. (2013). Initial stages of oceanic spreading in the Bransfield rift from magnetic and gravity data analysis. *Tectonophysics* 585, 102–112. doi:10.1016/j.tecto.2012.09.016

Catalán, M., Martos, Y. M., Martín-Davila, J., Muñoz-Martín, A., Carbó, A., and Druet, M. (2015). Radiografía de un margen continental utilizando campos potenciales y espesor de sedimentos: El Margen Atlántico Ibérico. *Bol. Geol. Min.* 126 (2–3), 515–532.

Choe, H., and Dyment, J. (2019). Fading magnetic anomalies, thermal structure and earthquakes in the Japan trench. *Geology* 48, 278–282. doi:10.1130/G46842.1

Coren, F., Ceccone, G., Lodolo, E., Zanolla, C., Zitellini, N., Bonazzi, C., et al. (1997). Morphology, seismic structure and tectonic development of the Powell basin, Antarctica. *J. Geol. Soc.* 154 (5), 849–862. doi:10.1144/gsjgs.154.5.0849

Cressie, N. (1990). The origins of kriging. *Math. Geol.* 22 (3), 239–252. doi:10.1007/bf00889887

Eagles, G., and Livermore, R. A. (2002). Opening history of Powell basin, Antarctic Peninsula. *Mar. Geol.* 185, 195–205. doi:10.1016/s0025-3227(02)00191-3

Galindo-Zaldívar, J., Jabaloy, A., Maldonado, A., and de Galdeano, C. S. (1996). Continental fragmentation along the south Scotia Ridge transcurrent plate boundary (NE Antarctic Peninsula). *Tectonophysics* 258, 275–301. doi:10.1016/0040-1951(95)00211-1

Garrett, S. W. (1990). Interpretation of reconnaissance gravity and aeromagnetic surveys of the Antarctic Peninsula. *J. Geophys. Res.* 95 (B5), 6759–6777. doi:10.1029/jb095ib05p06759

Ghidella, M. E., Yáñez, G., and LaBrecque, J. L. (2002). Revised tectonic implications for the magnetic anomalies of the western Weddell Sea. *Tectonophysics* 347, 65–86. doi:10.1016/s0040-1951(01)00238-4

Ghosh, N., Hall, S. A., and Casey, J. F. (1984). Seafloor spreading magnetic anomalies in the Venezuelan basin. *Geol. Soc. Am. Mem.* 162, 65–80. doi:10.1130/mem162-p65

Grauch, V. J. S., and Cordell, L. (1987). Limitations of determining density or magnetic boundaries from the horizontal gradient of gravity or pseudogravity data. *Geophysics* 52 (1), 118–121. doi:10.1190/1.1442236

Heine, C., Dietmar Müller, R., Steinberger, B., and Torsvik, T. H. (2008). Subsidence in intracontinental basins due to dynamic topography. *Phys. Earth Planet. Interior.* 171, 252–264. doi:10.1016/j.pepi.2008.05.008

Heine, C., and Müller, R. D., (2008). "The intracontinental basins (ICONS) atlas—applications in eastern Australia," in Eastern Australasian basins symposium III: Sydney. Perth, Australia: Petroleum Exploration Society of Australia, 275–290.

Henning, A. T., Sawyer, D. S., and Templeton, D. C. (2004). Exhumed upper mantle within the ocean-continent transition on the northern West Iberia margin: evidence from prestack depth migration and total tectonic subsidence analyses. *J. Geophys. Res.* 109, B0510310. doi:1029/2003JB002526

Jones, M., Sandwell, S., and Beaman, R. (2010). New Soundings for SRTM30_Plus V7.0. Fifth Annual GEBCO Bathymetric Science Day. Callao, Peru: IHO/IOc Committee for the General Bathymetric Charts of the Oceans (GEBCO).

Keating, P., and Sailhac, P. (2004). Use of the analytic signal to identify magnetic anomalies due to kimberlite pipes. *Geophysics* 69 (1), 180–190. doi:10.1190/1.1649386

King, E. C., and Barker, P. F. (1988). The margins of the south Orkney microcontinent. *J. Geol. Soc.* 145, 317–331. doi:10.1144/gsjgs.145.2.0317

King, E. C., Leitchenkov, G., Galindo-Zaldívar, J., Maldonado, A., and Lodolo, E. (1997). "Crustal structure and sedimentation in Powell basin," in *Geology and statigraphy of the Antarctic margin part 2 Antarctic research series*. Editors P. F. Barker and A. K. Cooper (Washington, DC: AGU), Vol. 71, 75–93.

Lawver, L. A., Williams, T., and Sloan, B. (1994). Seismic stratigraphy and heat flow of Powell basin. *Terra Antarct.* 1 (2), 309–310.

Levi, S., and Riddihough, R. (1986). Why are marine magnetic anomalies suppressed over sedimented spreading centers?. *Geology* 14, 651–654. doi:10.1130/0091-7613(1986)14<651:wammas>2.0.co;2

Livermore, R., Eagles, G., Morris, P., and Maldonado, A. (2004). Shackleton fracture zone: no barrier to early circumpolar ocean circulation. *Geology* 32, 797–800. doi:10.1130/g20537.1

Martos, Y. M., Catalán, M., Galindo-Zaldívar, J., Maldonado, A., and Bohoyo, F. (2014a). Insights about the structure and evolution of the Scotia Arc from a new magnetic data compilation. *Glob. Planet. Change.* 123, 239–248. doi:10.1016/j.gloplacha.2014.07.022

Martos, Y. M., Catalán, M., and Galindo-Zaldívar, J. (2019). Curie depth, heat flux and thermal subsidence studies reveal the Pacific mantle outflow through the Scotia Sea. *Jou. Geophy. Res.*: Solid Earth, 124. doi:10.1029/2019JB017677

Martos, Y. M., Galindo-Zaldívar, J., Catalán, M., Bohoyo, F., and Maldonado, A. (2014b). Asthenospheric Pacific–Atlantic flow barriers and the west Scotia ridge extinction. *Geophys. Res. Lett.* 41, 1–7. doi:10.1002/2013GL058885.

Martos, Y. M., Maldonado, A., Lobo, F. J., Hernández-Molina, F. J., and Pérez, L. F. (2013). Tectonics and palaeoceanographic evolution recorded by contourite features in southern Drake Passage (Antarctica). *Mar. Geol.* 343, 76–91. doi:10.1016/j.margeo.2013.06.015

Nettleton, L. L. (1976). *Gravity and magnetic in oil exploration*. New York, NY: Mac Graw-Hill.

Orihuela, N., García, A., and Arnaiz, M. (2013). Magnetic anomalies in the eastern Caribbean. *Int. J. Earth Sci.* 102, 591–604. doi:10.1007/s00531-012-0828-6

Quesnel, Y., Catalán, M., and Ishihara, T. (2009). A new global marine magnetic anomaly data set. *J. Geophys. Res.* 114, B04106. doi:10.1029/2008jb006144

Rodríguez-Fernández, J., Balanya, J.-C., Galindo-Zaldívar, J., and Maldonado, A. (1997). Tectonic evolution of a restricted ocean basin: the Powell basin (northeastern Antarctic Peninsula). *Geodin. Acta.* 10 (4), 159–174. doi:10.1080/09853111.1997.11105300

Roest, W. R., and Pilkington, M. (1993). Identifying remanent magnetization effects in magnetic data. *Geophysics* 58, 653–659. doi:10.1190/1.1443449

Roest, W. R., Verhoef, J., and Pilkington, M. (1992). Magnetic interpretation using the 3-D analytic signal. *Geophysics* 57, 116–125. doi:10.1190/1.1443174

Russell, S. M., and Whitmarsh, R. B. (2003). Magmatism at the west Iberia non-volcanic rifted continental margin: evidence from analyses of magnetic anomalies. *Geophys. J. Int.* 154, 706–730. doi:10.1046/j.1365-246X.2003.01999.x

Sabaka, T. J., Olsen, N., and Purucker, M. E. (2004). Extending comprehensive models of the Earth's magnetic field with Ørsted and CHAMP data. *Geophys. J. Int.* 159, 521–547. doi:10.1111/j.1365-246x.2004.02421.x

Salem, A., Ravat, D., Gamey, T. J., and Ushijima, K. (2002). Analytic signal approach and its applicability in environmental magnetic investigations. *J. Appl. Geophys.* 49, 231–244. doi:10.1016/s0926-9851(02)00125-8

Sandwell, D. T., Müller, R. D., Smith, W. H. F., García, E., and Francis, R. (2014). New global marine gravity model from CryoSat-2 and Jason-1 reveals buried tectonic structure. *Science* 346, 65–67. doi:10.1126/science.1258213

Sawyer, D. S. (1985). Total tectonic subsidence: a parameter for distinguishing crust type at the U.S. Atlantic continental margin. *J. Geophys. Res.* 90 (B9), 7751–7769. doi:10.1029/jb090ib09p07751

Schouten, H., Tivey, M. A., Fornari, D. J., and Cochran, J. R. (1999). Central anomaly magnetization high: constraints on the volcanic construction and architecture of seismic layer 2A at a fast-spreading mid-ocean ridge, the EPR at 9°30′–50′N. *Earth Planet Sci. Lett.* 169, 37–50. doi:10.1016/s0012-821x(99)00063-1

Sibuet, J.-C., Srivastava, S. P., and Spakman, W. (2004). Pyrenean orogeny and plate kinematics. *J. Geophys. Res.* 109, 1–18. doi:10.1029/2003JB002514

Suriñach, E., Galindo-Zaldívar, J., Maldonado, A., and Livermore, R. (1997). Large amplitude magnetic anomalies in the northern sector of the Powell basin, NE Antarctic Peninsula. *Mar. Geophys. Res.* 19, 65–80. doi:10.1023/A:1004240931967

Sykes, T. J. S. (1996). A correction for sediment load upon the ocean floor: uniform versus varying sediment density estimations-implications for isostatic correction. *Mar. Geol.* 133, 35–49. doi:10.1016/0025-3227(96)00016-3

Tivey, M. A., and Johnson, H. P. (1993). Variations in oceanic crustal structure and implications for the fine-scale magnetic anomaly signal. *Geophys. Res. Lett.* 20 (17), 1879–1882. doi:10.1029/93gl01485

Zhou, W., Van der Voo, R., Peacor, D. R., Wang, D., and Zhang, Y. (2001). Low-temperature oxidation in MORB of titanomagnetite to titanomaghemite: a gradual process with implications for marine magnetic anomaly amplitudes. *J. Geophys. Res.* 106, 6409–6421. doi:10.1029/2000JB900447

Conflict of Interest: The authors declare that the research was conducted in the absence of any commercial or financial relationships that could be construed as a potential conflict of interest.